



Titanium Phosphate Nanoplates Modified With AgBr@Ag Nanoparticles: A Novel Heterostructured Photocatalyst With Significantly Enhanced Visible Light Responsive Activity

Manli Ren, Jiaqiu Bao, Peifang Wang, Chao Wang and Yanhui Ao*

Key Laboratory of Integrated Regulation and Resource Development on Shallow Lakes, Ministry of Education, College of Environment, Hohai University, Nanjing, China

OPEN ACCESS

Edited by:

Fan Dong,
Chongqing Technology and Business
University, China

Reviewed by:

Guohong Wang,
Hubei Normal University, China
Qizhao Wang,
Northwest Normal University, China

*Correspondence:

Yanhui Ao
andyao@hhu.edu.cn

Specialty section:

This article was submitted to
Catalysis and Photocatalysis,
a section of the journal
Frontiers in Chemistry

Received: 17 July 2018

Accepted: 25 September 2018

Published: 17 October 2018

Citation:

Ren M, Bao J, Wang P, Wang C and
Ao Y (2018) Titanium Phosphate
Nanoplates Modified With AgBr@Ag
Nanoparticles: A Novel
Heterostructured Photocatalyst With
Significantly Enhanced Visible Light
Responsive Activity.
Front. Chem. 6:489.
doi: 10.3389/fchem.2018.00489

AgBr@Ag modified titanium phosphate composites were fabricated through a two-step approach. The prepared samples were characterized by X-ray diffraction, scanning electron microscopy, and transmission electron microscopy. The optical properties of the composites were characterized by using UV-vis diffuse reflectance spectroscopy. The photocatalytic activities of the composites were investigated on the degradation of Rhodamine B and ciprofloxacin under visible light irradiation. AgBr@Ag/titanium phosphate was determined to exhibit considerably higher photocatalytic activity than the corresponding individual components. The mechanism on the enhancement of the photocatalytic activity was proposed based on the results of photoluminescence spectra and photocurrent measurements. Furthermore, the possible photocatalytic mechanisms of organic compounds degradation were also proposed.

Keywords: heterojunction, titanium phosphate, AgBr@Ag, photocatalysis, visible light

INTRODUCTION

Environmental pollution has become a global problem due to the accelerated development of human society (Ye et al., 2012; Sun et al., 2017; Zhang et al., 2017; Li et al., 2018a; Lu et al., 2018). Therefore, it is urgent to solve this severe problem via green technology (Liu et al., 2012; Hao et al., 2016; Zou et al., 2016; Chen et al., 2018; Feng et al., 2018; Guo et al., 2018). Currently, photocatalysis technology has received intense attention as an efficient technology for solving the problem of environment (Fan et al., 2013; Ao et al., 2016; Wang et al., 2016; Dong et al., 2017; Hao et al., 2017). Furthermore, it is well known that composite photocatalysts always show higher activity than the corresponding single component (Ma et al., 2018; Wang et al., 2018; Zhang et al., 2018). The improved photocatalytic activity is due to the different electronic energy levels of different components, which create an internal electric field that can accelerate the separation rate of photogenerated electrons and holes, and reduce their recombination rate (Guo et al., 2017).

Recently, titanium phosphate has been widely studied for the treatment of organic compounds. Titanium phosphate [α -Ti(HPO₄)₂•H₂O, hereafter TP] consists of layers of titanium atoms bonding on both plane sides of the monohydrogen phosphate groups. Water molecules located in

the interlayer region to form a network of hydrogen-bonding with phosphate groups (Ekambaram et al., 2000; Guo et al., 2013; Guo and Han, 2014; Zhu et al., 2014). However, titanium phosphate can only absorb ultraviolet light (<5% of the sunlight). Furthermore, the high recombination rate of photoinduced electron-hole pairs is still exist, which would lead to lower

photocatalytic activity. Thus, it is urgent to find effective ways to improve the activity of the TP.

Recently, silver halide materials have received intense attention due to their excellent visible light responsive photocatalytic activity. Silver halide@silver nanoparticles (AgNPs) based heterojunctions have been found to be excellent photocatalysts (Chen et al., 2015; Bai et al., 2016; Li et al., 2018b; Xuan et al., 2018). It has been proved that plasmon AgNPs on the surface of AgX can enhance the light absorption of the composites and accelerate the separation rate of the photogenerated charges (Daupor and Wongnawa, 2014; Li et al., 2015a,b; Ding et al., 2018; Xiao et al., 2018). Moreover, it was also considered that AgNPs decrease the recombination rate of Ag^+ with photogenerated electrons, and allow the formation of Br^0 species (photogenerated holes react with Br^- ions) that can degrade the organic compounds (Xia and Halas, 2005; Jiang et al., 2014; Zhang et al., 2015a). Therefore, it would be a good way to obtain higher visible light activated activity through the combination of AgBr@Ag and TP.

In this work, we prepared visible light active AgBr@Ag/TP photocatalysts by a simple and feasible method. The morphology, crystal structure, optical properties, and composition of the photocatalysts were investigated. Moreover, the possible photocatalytic degradation mechanism of ciprofloxacin and the enhancement mechanism photocatalytic activity were proposed.

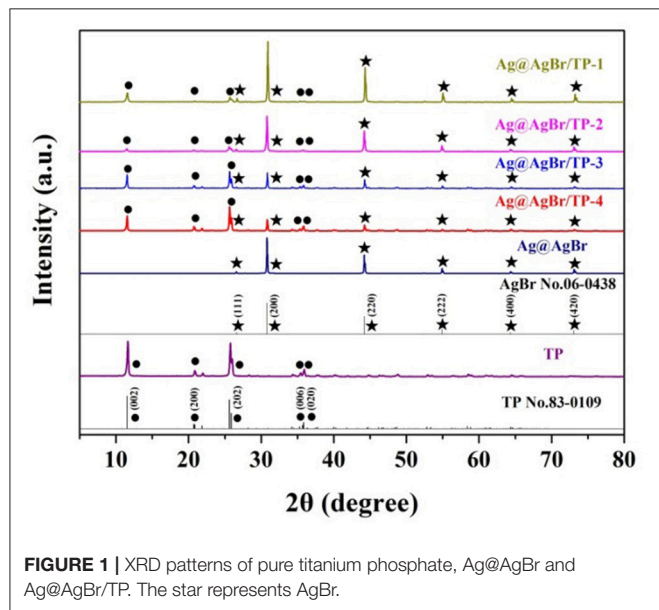


FIGURE 1 | XRD patterns of pure titanium phosphate, Ag@AgBr and Ag@AgBr/TP. The star represents AgBr.

EXPERIMENTAL

All experimental details are shown in **Supporting Information**.

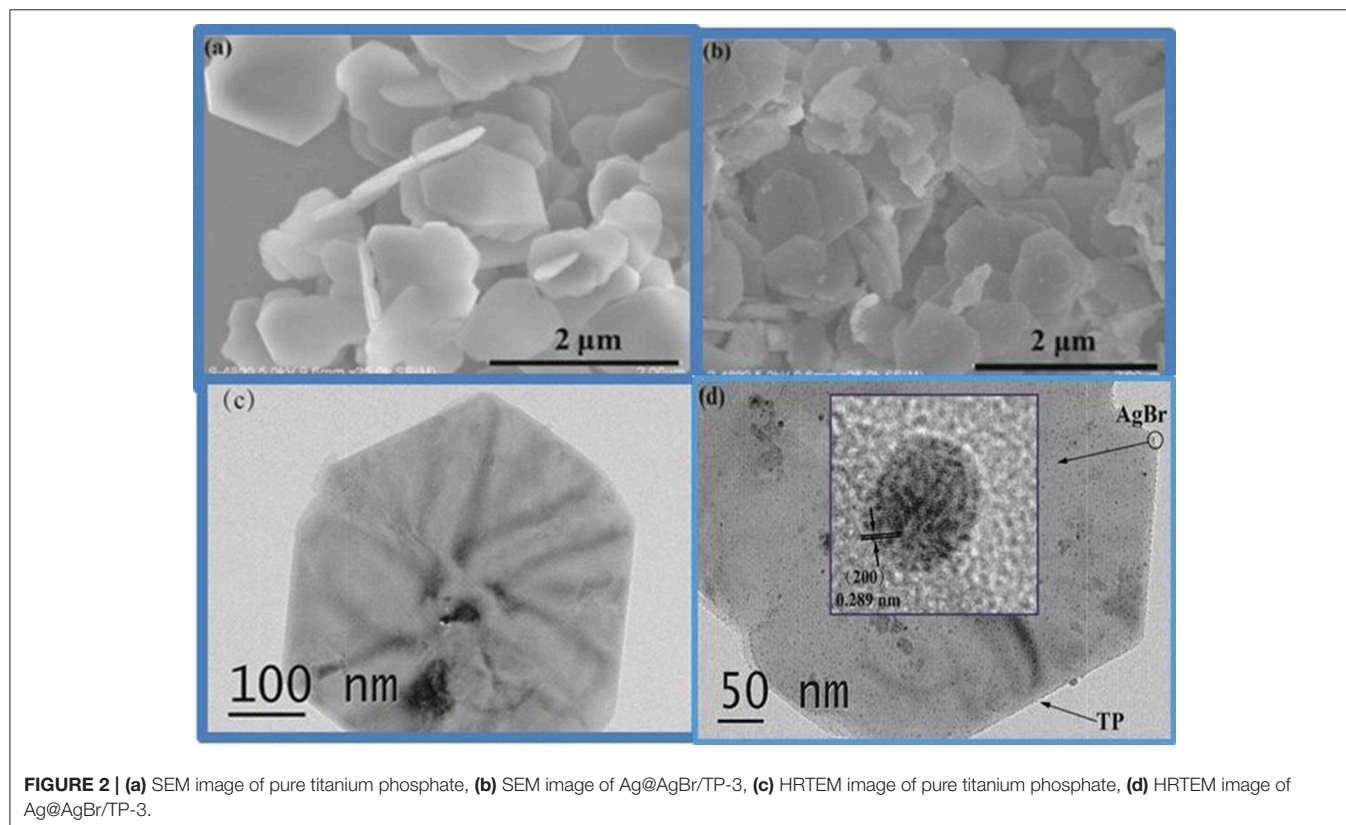


FIGURE 2 | (a) SEM image of pure titanium phosphate, (b) SEM image of Ag@AgBr/TP-3, (c) HRTEM image of pure titanium phosphate, (d) HRTEM image of Ag@AgBr/TP-3.

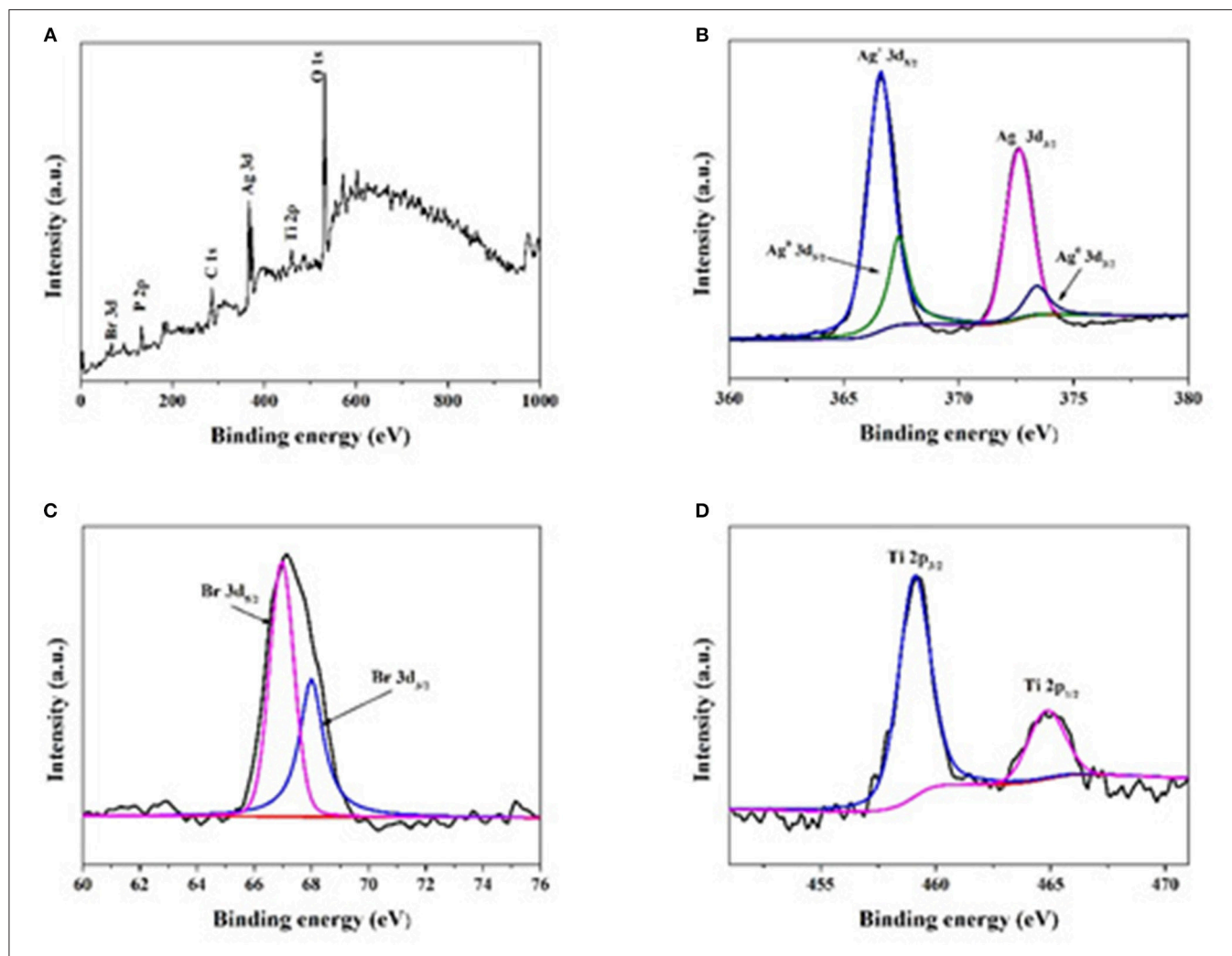


FIGURE 3 | XPS spectra of Ag@AgBr/TP-3. **(A)** The survey XPS spectrum, **(B)** Ag 3d, **(C)** Br 3d, **(D)** Ti 2p peaks related to the photocatalyst.

RESULTS AND DISCUSSION

Characterization

The phase structure was characterized by XRD, and the obtained patterns are shown in **Figure 1**. The peaks at about 11.6, 21.0, 26.0, 35.4, and 35.8° are indexed to the (002), (200), (202), (006), and (020) directions, respectively. All peaks can be ascribed to TP (JCPDS Card No: 83-0109; Ortíz-Oliveros et al., 2014; Yada et al., 2014). Diffraction peaks are also detected at 26.73, 30.96, 44.35, 55.04, 64.49, and 73.26°, which can be indexed to the (111), (200), (220), (222), (400), and (420) directions of AgBr (JCPDS Card NO: 06-0438; Chen et al., 2015; Bai et al., 2016). Furthermore, with the increasing of AgBr mass, the intensity of the characteristic peaks of AgBr increased gradually. No diffraction peaks of Ag can be observed, possibly due to its low mass, high dispersion or small size (Wang et al., 2013, 2014).

The morphologies of the composites were investigated by TEM and SEM. The obtained SEM image of pure TP is displayed in **Figure 2a**. It can be seen that the TP sample is composed

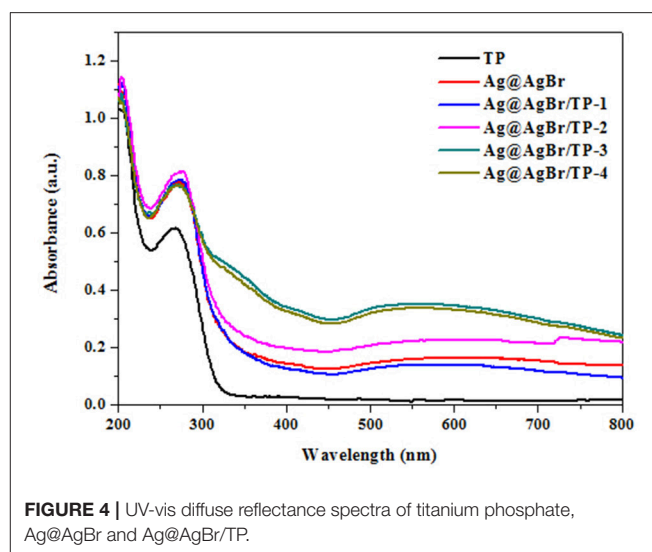
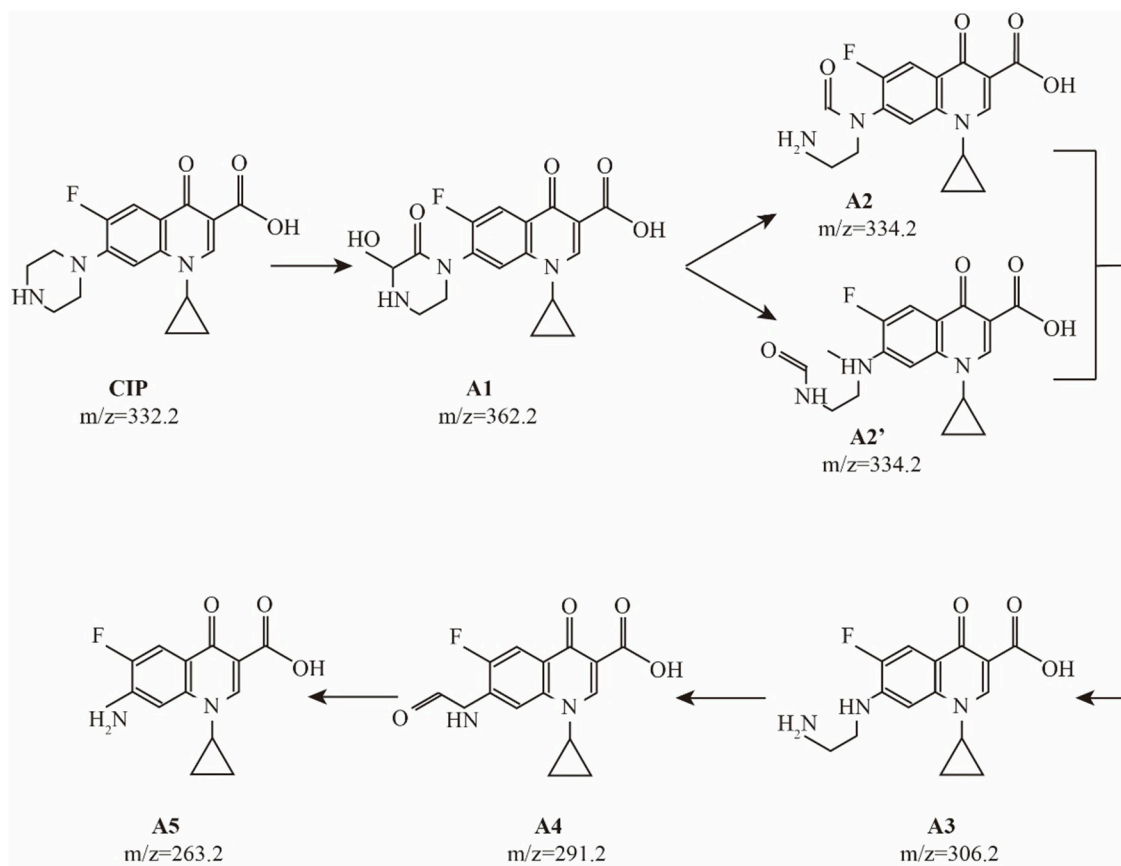
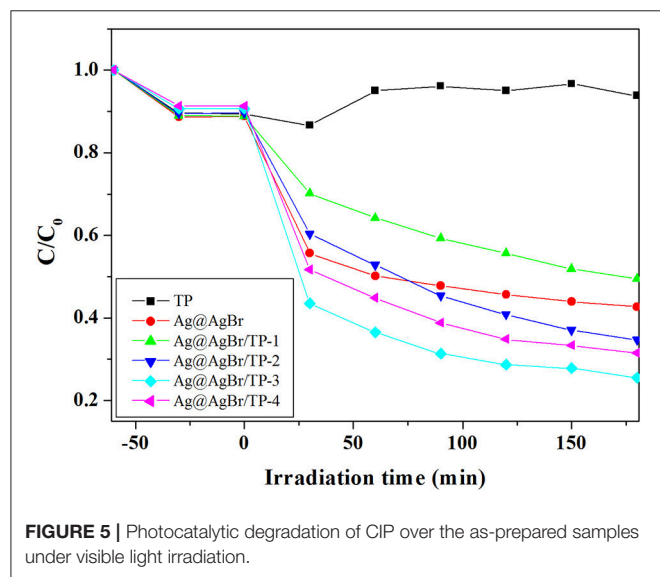


FIGURE 4 | UV-vis diffuse reflectance spectra of titanium phosphate, Ag@AgBr and Ag@AgBr/TP.

of uniform plates with sub-micrometer width and 30~40 nm thickness. The SEM image of AgBr@Ag/TP-3 taken from **Figure 2b** displays smaller AgBr@Ag nanoparticles decorating

the TP surface. The TEM image of pure TP is displayed in **Figure 2c**. It can also be seen that the titanium phosphate plate is hexagonal, which is in good agreement with the results of SEM. The TEM image of AgBr@Ag/TP is shown in **Figure 2d**. It can be seen that AgBr nanoparticles decorated the TP surface, indicating the formation of heterojunctions in the prepared samples (Cui et al., 2018). As shown in the inset of **Figure 2d**, the measured lattice spacings of 0.289 nm corresponds to the (200) lattice planes of AgBr.

The elemental composition and chemical states of the elements in the composites were analyzed by XPS. The peaks of Br 3d, P 2p, Ag 3d, C 1s, Ti 2p, and O 1s can be observed in **Figures 3A,B** shows the electron binding energies of Ag 3d_{5/2} and Ag 3d_{3/2} orbitals, which can be further divided into 366.6/367.4 and 372.6/373.4 eV, respectively. The peaks at 366.6 and 372.6 eV indicate the presence of Ag⁺. Both the peak separation (6.0 eV) and peak positions (367.4 and 373.4 eV) indicate the presence of metallic form (Ag⁰; Yang et al., 2015; Tang et al., 2017a,b). As shown in **Figure 3C**, two peaks at 68.0 and 67.0 eV corresponding to the binding energies of Br 3d_{3/2} and Br 3d_{5/2} can be found (Wang et al., 2009). All above results prove the presence of AgBr and Ag in the composite. In **Figure 3D**, the Ti peaks observed at 459.0 and

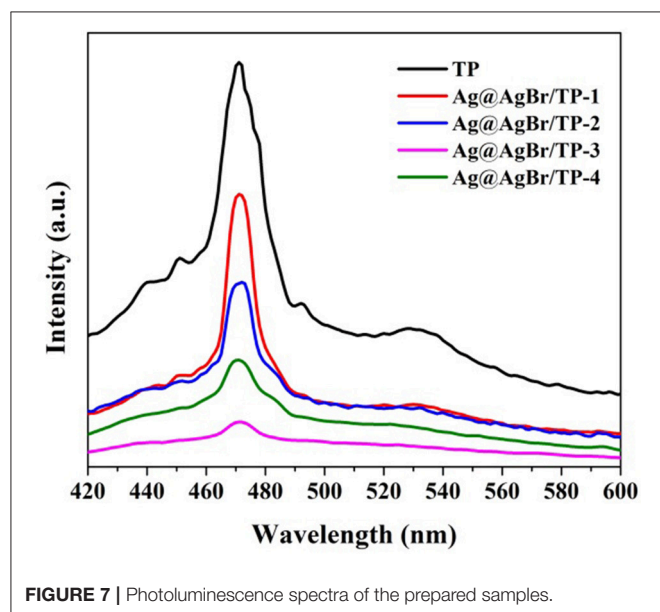


464.8 eV can be attributed to Ti 2p_{3/2} and Ti 2p_{1/2}. The peak separation of 5.8 eV for binding energy between the two peaks indicates that Ti was mainly Ti⁴⁺ in the composite (Yada et al., 2014).

The optical properties of photocatalysts significantly affect their photocatalytic performance (He et al., 2015). Therefore, optical properties of the composites were investigated by DRS and the obtained results are shown in **Figure 4**. Pure TP exhibited no absorption in the visible-light region, whereas the Ag@AgBr/TP composites had better absorption performance, possibly due to the deposition of AgBr and formation of AgNPs on the surface of the composites. Moreover, Ag@AgBr/TP-3 showed the highest absorption in visible light region, indicating that high absorption capability is ascribed to an optimal loading. In other words, when the loading of AgBr@Ag exceeds a critical value, the AgBr@Ag nanoparticles would agglomerate and decrease the absorption capability.

Photocatalytic Activity

To investigate the photocatalytic performance of the composites, we conducted experiments on the degradation of colorless organic pollutant (CIP) under visible light irradiation. As shown in **Figure 5**, AgBr@Ag/TP-3 displayed the highest photocatalytic activity for CIP degradation among all samples. Approximately 51.4, 44.2, 61.3, 71.5, and 65.4% of CIP was degraded in 180 min by AgBr@Ag, AgBr@Ag/TP-1, AgBr@Ag/TP-2, AgBr@Ag/TP-3, and AgBr@Ag/TP-4, respectively. Furthermore, the TP showed a low photocatalytic efficiency for CIP degradation. The degradation curve of CIP by TP exhibits a fluctuating trend. There may be some CIP molecules desorbed from the surface of TP. These results show that the Ag@AgBr/TP photocatalysts are generally effective for the degradation of colorless organic compounds.

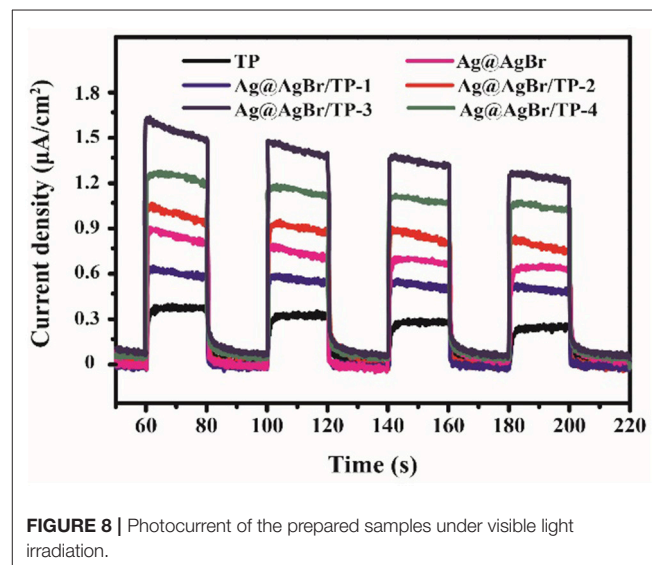


Intermediates Analysis

Prior to the complete mineralization of CIP, there are many degradation intermediates in the photocatalytic process. The sample solution was detected by HPLC/MS during the photocatalytic degradation. Some intermediates in the photocatalytic process were identified: A1 (*m/z* = 362.2), A2 (*m/z* = 334.2), A3 (*m/z* = 306.2), A4 (*m/z* = 291.2), and A5 (*m/z* = 263.2). These results show that A1~A5 are the main intermediates during the degradation process of CIP. As observed in many other oxidation system (Sturini et al., 2012), desethyleneciprofloxacin (A3) was dominant intermediate of CIP, and was formed by a net loss of C₂H₂ at the piperazinyl substituent of CIP. Prior to the formation of desethyleneciprofloxacin, two intermediates were detected. The hydroxyl keto-derivative of the piperazinyl substituent (A1) was detected to be the first oxidized intermediate on the way to the formation of A3. Apparently, the subsequent loss of CO from A1 results in the cleavage of the piperazinyl ring to form keto-derivatives A2 and A2', in which a carbonyl group remains on the N atom of aniline and alkylamine, respectively. A second loss of a CO molecule from A2 and A2' leads to the formation of desethyleneciprofloxacin (A3). The further oxidation of desethyleneciprofloxacin (A3) generated A4 with a keto group through the loss of a N atom. The decarbonylation of A4 forms aniline (A5), completely destroying the piperazinyl substituent of CIP. The probable pathways for CIP degradation are shown in **Figure 6**.

Possible Photocatalytic Mechanism

Several experiments were performed to further understand the mechanism on the enhancement of photocatalytic performance for the AgBr@Ag/TP composites. The photoluminescence (PL) spectrum was measured to investigate the recombination rate of the photogenerated electron-hole pairs. The photoluminescence spectra of the prepared samples are shown in **Figure 7**. The intensity of PL is directly proportional to the electron-hole



recombination rate, and lower PL intensity means lower recombination rate (Zhang et al., 2015b; Shi et al., 2016). The main emission peak of pure TP centers at ~ 470 nm, which was ascribed to the band gap recombination of electron-hole pairs. The PL intensity decreases significantly after the deposition of AgBr@Ag. The decreasing emission intensity of the AgBr@Ag/TP suggests that the recombination of electron-hole pairs can be suppressed after the deposition of AgBr@Ag (Xu et al., 2013). Furthermore, it can be seen that the PL intensity increase as the amount of Ag@AgBr increase to a certain value, and AgBr@Ag/TP-3 composite showed the lowest PL intensity, which means Ag@AgBr/TP-3 composite has the lowest recombination rate of photogenerated electrons-hole pairs. Therefore, it would lead to the highest photocatalytic performance. However, the PL intensity increase as the amount of Ag@AgBr increase further. It can be ascribed to the reason that superfluous Ag@AgBr nanoparticles would aggregate thus cannot form effective heterojunctions with TP. The above results demonstrate that the deposition of AgBr on TP and the formation of AgNPs on the surface of the composite can decrease the recombination efficiency and enhance the separation efficiency of the photogenerated electrons and holes.

It is well known that the efficiency of the electron-hole pairs separation significantly affects the photocatalytic performance (Jiang et al., 2011). The electrons in the valence band of photocatalysts can be activated and then transfer to the conduction band, leading to the formation of photocurrent. A higher photocurrent means higher electron-hole pairs separation rate, which induces to better photocatalytic performance (Xiang et al., 2011). **Figure 8** shows the photocurrents for different samples under 20 s intermittent visible-light irradiation with a bias of 0.3 V. The photocurrents of AgBr@Ag/TP composites are all much higher than that of TP. Moreover, AgBr@Ag/TP-3 exhibits the highest value. The results are in good agreement

with the photocatalytic activity, indicating that the efficient separation of photo-induced electrons and holes results in the high photocatalytic activity.

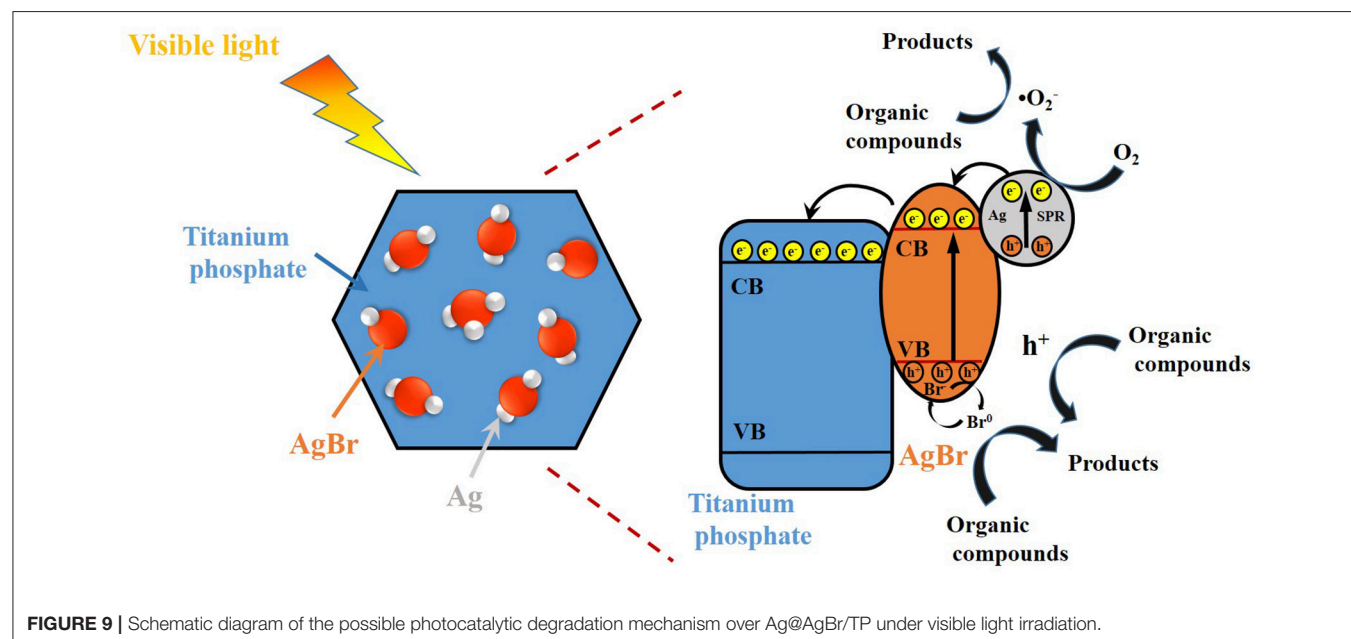
It was demonstrated that the separation efficiency of photo-generated electrons and holes is important to the photocatalytic performance. Furthermore, the conduction band (CB) and valence band (VB) potential have a significantly effect on the separation of the photogenerated electron-hole pairs. The CB and VB potential of AgBr and TP can be obtained using Equations. (1) and (2) (Zhang et al., 2008):

$$E_{vb} = X - E_0 + 0.5E_g \quad (1)$$

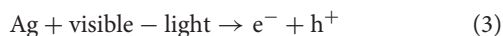
$$E_{cb} = E_{vb} - E_g \quad (2)$$

where E_{vb} is the potential of VB, X is the absolute electronegativity of photocatalyst (X is 6.85 eV and 5.81 eV of TP and AgBr, respectively), E_g is the band gap energy and E_0 is the energy of free electrons (~ 4.5 eV). Based on these equations, the CB potential (E_{cb}) and VB potential (E_{vb}) of TP are calculated as 0.43 and 4.28 eV, while E_{cb} and E_{vb} of AgBr are calculated as 0.01 eV and 2.62 eV, respectively.

Therefore, a possible mechanism on the photocatalytic degradation of RhB by AgBr@Ag/TP under the irradiation of visible light is illustrated in **Figure 9**. The plasmon induced holes can react with Br^- and form active Br^0 atoms. The Br^0 atoms exhibit an excellent oxidation capability to oxidize organic compounds. Meanwhile, plasmon induced electrons are formed on the surface of AgNPs, part of these electrons are trapped by O_2 to produce $\bullet\text{O}_2^-$, mainly contributing to the organic compounds removal (Ye et al., 2012; Zhang and Yates, 2012; Cheng et al., 2015; Ding et al., 2018). Besides, the other electrons would transfer to the conduction band of AgBr, and then further transfer from AgBr to the conduction band of TP. Meanwhile, the h^+



stored in valence band of AgBr and TP was also involved in the organic compounds photocatalytic degradation, though they are not the dominant active species. The relevant equations are shown as following:



Based on above results, the possible mechanism on the enhancement of photocatalytic activity for AgBr@Ag/TP composites can be proposed. AgBr@Ag nanoparticles deposited on TP improve the light absorption capability, as confirmed by UV-vis DRS studies. Furthermore, the heterojunctions between AgNPs, AgBr, and TP are conducive to improving the transfer rate and separation efficiency of the electron-hole pairs, and hindering the recombination of the pairs, thus inducing to the enhancement of the photocatalytic activity.

CONCLUSIONS

AgBr@Ag/TP composites exhibited higher photocatalytic performance than pure TP and AgBr@Ag, and can degrade a

typical antibiotic (CIP) under the irradiation of visible light. The excellent photocatalytic activity can be ascribed to their enhanced visible-light absorption, low recombination and high transferring rate of the photo-generated charges, as shown by DRS, PL, and photocurrent experiments.

AUTHOR CONTRIBUTIONS

YA and CW designed the project and guided the work. MR and JB conducted the experiments and characterizations of the samples. PW revised and polished the manuscript.

ACKNOWLEDGMENTS

We are grateful for grants from National Science Funds for Creative Research Groups of China (No. 51421006), Natural Science Foundation of China (51679063), the Fundamental Research Funds for The Central Universities (2018B14514), the Key Program of National Natural Science Foundation of China (No. 91647206), the National Key Plan for Research and Development of China (2016YFC0502203), and PAPD.

SUPPLEMENTARY MATERIAL

The Supplementary Material for this article can be found online at: <https://www.frontiersin.org/articles/10.3389/fchem.2018.00489/full#supplementary-material>

REFERENCES

- Ao, Y., Wang, K., Wang, P., Wang, C., and Hou, J. (2016). Synthesis of novel 2D-2D p-n heterojunction BiOBr/La₂Ti₂O₇ composite photocatalyst with enhanced photocatalytic performance under both UV and visible light irradiation. *Appl. Catal. B-Environ.* 194, 157–168. doi: 10.1016/j.apcatb.2016.04.050
- Bai, Y. Y., Lu, Y., and Liu, J. K. (2016). An efficient photocatalyst for degradation of various organic dyes: Ag@Ag₂MoO₄-AgBr composite. *J. Hazard. Mater.* 307, 26–35. doi: 10.1016/j.jhazmat.2015.12.052
- Chen, D., Wang, Z., Du, Y., Yang, G., Ren, T., and Ding, H. (2015). *In situ* ionic-liquid-assisted synthesis of plasmonic photocatalyst Ag/AgBr/g-C₃N₄ with enhanced visible-light photocatalytic activity. *Catal. Today.* 258, 41–48. doi: 10.1016/j.cattod.2015.03.031
- Chen, P., Dong, F., Ran, M., and Li, J. (2018). Synergistic photo-thermal catalytic NO purification of MnOx/g-C₃N₄: enhanced performance and reaction mechanism. *Chin. J. Catal.* 39, 619–629. doi: 10.1016/S1872-2067(18)63029-3
- Cheng, Z., Wang, Z., Shifa, T. A., Wang, F., Zhan, X., Xu, K., et al. (2015). Au plasmonics in a WS₂-Au-CuInS₂ photocatalyst for significantly enhanced hydrogen generation. *Appl. Phys. Lett.* 107, 253–278. doi: 10.1063/1.4937008
- Cui, X., Tian, L., Xian, X., Tang, H., and Yang, X. (2018). Solar photocatalytic water oxidation over Ag₃PO₄/g-C₃N₄ composite materials mediated by metallic Ag and graphene. *Appl. Surf. Sci.* 430, 108–115. doi: 10.1016/j.apsusc.2017.07.290
- Daupor, H., and Wongnawa, S. (2014). Urchinlike Ag/AgCl photocatalyst: synthesis, characterization, and activity. *Appl. Catal. A-Gen.* 473, 59–69. doi: 10.1016/j.apcata.2013.12.036
- Ding, K., Yu, D., Wang, W., Gao, P., and Liu, B. (2018). Fabrication of multiple hierarchical heterojunction Ag@AgBr/BiPO₄/r-GO with enhanced visible-light-driven photocatalytic activities towards dye degradation. *Appl. Surf. Sci.* 445, 39–49. doi: 10.1016/j.apsusc.2018.03.131
- Dong, W. H., Wu, D. D., Luo, J. M., Xing, Q. J., Liu, H., Zou, J. P., et al. (2017). Coupling of photodegradation of RhB with photoreduction of CO₂ over rGO/SrTi_{0.95}Fe_{0.05}O_{3-δ} catalyst: a strategy for one-pot conversion of organic pollutants to methanol and ethanol. *J. Catal.* 349, 218–225. doi: 10.1016/j.jcat.2017.02.004
- Ekambaram, S., Christian, S., Serre, Gérard Férey, a. and Slavi, C., Sevov (2000). Hydrothermal synthesis and characterization of an ethylenediamine-templated mixed-valence titanium phosphate. *Chem. Mater.* 31, 444–449. doi: 10.1021/cm990492i
- Fan, W., Zhang, Q., and Wang, Y. (2013). Semiconductor-based nanocomposites for photocatalytic H₂ production and CO₂ conversion. *Phys. Chem. Chem. Phys.* 15, 2632–2649. doi: 10.1039/c2cp43524a
- Feng, X.Y., Wang, P.F., Hou, J., Qian, J., Wang, C., and Ao, Y. H. (2018). Oxygen vacancies and phosphorus codoped black titania coated carbon nanotube composite photocatalyst with efficient photocatalytic performance for the degradation of acetaminophen under visible light irradiation. *Chem. Engin. J.* 352: 947–956. doi: 10.1016/j.cej.2018.06.037
- Guo, H., Niu, C. G., Wen, X. J., Zhang, L., Liang, C., Zhang, X. G., et al. (2017). Construction of highly efficient and stable ternary AgBr/Ag/PbBiO₂Br Z-scheme photocatalyst under visible light irradiation: performance and mechanism insight. *J. Colloid Interface Sci.* 513, 852–865. doi: 10.1016/j.jcis.2017.12.010
- Guo, S. Y., and Han, S. (2014). Constructing a novel hierarchical 3D flower-like nano/micro titanium phosphate with efficient hydrogen evolution from water splitting. *J. Power Sources.* 267, 9–13. doi: 10.1016/j.jpowsour.2014.05.011
- Guo, S. Y., Han, S., Chi, B., Pu, J., and Li, J. (2013). Synthesis of shape-controlled mesoporous titanium phosphate nanocrystals: the hexagonal titanium phosphate with enhanced hydrogen generation from water splitting. *Int. J. Hydrogen Energy* 39, 2446–2453. doi: 10.1016/j.ijhydene.2013.12.007
- Guo, Y., Wang, P., Qian, J., Ao, Y., Wang, C., and Hou, J. (2018). Phosphate group grafted twinned BiPO₄ with significantly enhanced photocatalytic activity:

- synergistic effect of improved charge separation efficiency and redox ability. *Appl. Catal. B-Environ.* 234, 90–99. doi: 10.1016/j.apcatb.2018.04.036
- Hao, R., Wang, G., Jiang, C., Tang, H., and Xu, Q. (2017). In situ hydrothermal synthesis of g-C₃N₄/TiO₂ heterojunction photocatalysts with high specific surface area for Rhodamine B degradation. *Appl. Surf. Sci.* 411, 400–410. doi: 10.1016/j.apsusc.2017.03.197
- Hao, R., Wang, G., Tang, H., Sun, L., Xu, C., and Han, D. (2016). Template-free preparation of macro/mesoporous g-C₃N₄/TiO₂ heterojunction photocatalysts with enhanced visible light photocatalytic activity. *Appl. Catal. B-Environ.* 187, 47–58. doi: 10.1016/j.apcatb.2016.01.026
- He, Y., Wang, Y., Zhang, L., Teng, B., and Fan, M. (2015). High-efficiency conversion of CO₂ to fuel over ZnO/g-C₃N₄ photocatalyst. *Appl. Catal. B-Environ.* 168, 1–8. doi: 10.1016/j.apcatb.2014.12.017
- Jiang, J., Zhang, X., Sun, P., and Zhang, L. (2011). ZnO/BiOI heterostructures: photoinduced charge-transfer property and enhanced visible-light photocatalytic activity. *J. Phys. Chem.* 115, 20555–20564. doi: 10.1021/jp205925z
- Jiang, R., Li, B., Fang, C., and Wang, J. (2014). Metal/semiconductor hybrid nanostructures for plasmon-enhanced applications. *Adv. Mater.* 26, 5274–5309. doi: 10.1002/adma.201400203
- Li, S., Hu, S., Jiang, W., Liu, Y., Liu, Y., Zhou, Y., et al. (2018a). Ag₃VO₄ nanoparticles decorated Bi₂O₂CO₃ micro-flowers: an efficient visible-light-driven photocatalyst for the removal of toxic contaminants. *Front. Chem.* 6:255. doi: 10.3389/fchem.2018.00255
- Li, S., Jiang, W., Hu, S., Liu, Y., and Liu, J. (2018b). Construction of a novel ternary Ag/AgBr/Ag₂WO₄ composite for efficient photocatalytic removal of Rhodamine B dye and tetracycline hydrochloride antibiotic. *Mater. Lett.* 224, 29–32. doi: 10.1016/j.matlet.2018.04.071
- Li, W., Ma, Z., Bai, G., Hu, J., Guo, X., Dai, B., et al. (2015a). Dopamine-assisted one-step fabrication of Ag@AgCl nanophotocatalyst with tunable morphology, composition and improved photocatalytic performance. *Appl. Catal. B-Environ.* 174, 43–48. doi: 10.1016/j.apcatb.2015.02.029
- Li, X., Fang, S., Ge, L., Han, C., Qiu, P., and Liu, W. (2015b). Synthesis of flower-like Ag/AgCl-Bi₂MoO₆ plasmonic photocatalysts with enhanced visible-light photocatalytic performance. *Appl. Catal. B-Environ.* 176–177, 62–69. doi: 10.1016/j.apcatb.2015.03.042
- Liu, R., Wang, P., Wang, X., Yu, H., and Yu, J. (2012). UV- and visible-light photocatalytic activity of simultaneously deposited and doped Ag/Ag(I)-TiO₂ photocatalyst. *J. Phys. Chem. C* 116, 17721–17728. doi: 10.1021/jp305774n
- Lu, L., Wang, G., Zou, M., Wang, J., and Li, J. (2018). Effects of calcining temperature on formation of hierarchical TiO₂/g-C₃N₄ hybrids as an effective Z-scheme heterojunction photocatalyst. *Appl. Surf. Sci.* 441, 1012–1023. doi: 10.1016/j.apsusc.2018.02.080
- Ma, L., Wang, G., Jiang, C., Bao, H., and Xu, Q. (2018). Synthesis of core-shell TiO₂@g-C₃N₄ hollow microspheres for efficient photocatalytic degradation of rhodamine B under visible light. *Appl. Surf. Sci.* 430, 263–272. doi: 10.1016/j.apsusc.2017.07.282
- Ortiz-Oliveros, H. B., Flores-Espinosa, R. M., Ordoñez-Regil, E., and Fernández-Valverde, S. M. (2014). Synthesis of α-Ti(HPO₄)₂·H₂O and sorption of Eu (III). *Chem. Eng. J.* 236, 398–405. doi: 10.1016/j.cej.0.2013.09.103
- Shi, W., Lv, H., Yuan, S., Huang, H., Liu, Y., and Kang, Z. (2016). Near-infrared light photocatalytic ability for degradation of tetracycline using carbon dots modified Ag/AgBr nanocomposites. *Sep. Purif. Technol.* 174, 75–83. doi: 10.1016/j.seppur.2016.10.005
- Sturini, M., Speltini, A., Maraschi, F., Profumo, A., Pretali, L., Irastorza, E. A., et al. (2012). Photolytic and photocatalytic degradation of fluoroquinolones in untreated river water under natural sunlight. *Appl. Catal. B-Environ.* 119–120, 32–39. doi: 10.1016/j.apcatb.2012.02.008
- Sun, Y., Xiao, X., Dong, X. A., Dong, F., and Zhang, W. (2017). Heterostructured BiOI@La(OH)₃ nanorods with enhanced visible light photocatalytic NO removal. *Chin. J. Catal.* 38, 217–226. doi: 10.1016/S1872-2067(17)62753-0
- Tang, H., Chang, S., Tang, G., and Liang, W. (2017a). AgBr and g-C₃N₄ co-modified Ag₂CO₃ photocatalyst: a novel multi-heterostructured photocatalyst with enhanced photocatalytic activity. *Appl. Surf. Sci.* 391, 440–448. doi: 10.1016/j.apsusc.2016.07.021
- Tang, H., Fu, Y., Chang, S., Xie, S., and Tang, G. (2017b). Construction of Ag₃PO₄/Ag₂MoO₄ Z-scheme heterogeneous photocatalyst for the remediation of organic pollutants. *Chin. J. Catal.* 38, 337–347. doi: 10.1016/S1872-2067(16)62570-6
- Wang, J., Wang, G., Wei, X., Liu, G., and Li, J. (2018). ZnO nanoparticles implanted in TiO₂ macrochannels as an effective direct Z-scheme heterojunction photocatalyst for degradation of RhB. *Appl. Surf. Sci.* 456, 666–675. doi: 10.1016/j.apsusc.2018.06.182
- Wang, P., Huang, B., Qin, X., Zhang, X., Dai, Y., and Whangbo, M. H. (2009). Ag/AgBr/WO₃·H₂O: visible-light photocatalyst for bacteria destruction. *Inorg. Chem.* 48, 10697–10702. doi: 10.1021/ic9014652
- Wang, Q., Yun, G., Bai, Y., Ning, A. N., Lian, J., Huang, H., et al. (2014). Photodegradation of rhodamine B with MoS₂/Bi₂O₂CO₃ composites under UV light irradiation. *Appl. Surf. Sci.* 313, 537–544. doi: 10.1016/j.apsusc.2014.06.018
- Wang, W., Cheng, H., Huang, B., Lin, X., Qin, X., Zhang, X., et al. (2013). Synthesis of Bi₂O₂CO₃/Bi₂S₃ hierarchical microspheres with heterojunctions and their enhanced visible light-driven photocatalytic degradation of dye pollutants. *J. Colloid Interface Sci.* 402, 34–39. doi: 10.1016/j.jcis.2013.03.054
- Wang, X., Li, T., Yu, R., Yu, H., and Yu, J. (2016). Highly efficient TiO₂ single-crystal photocatalyst with spatially separated Ag and F-biocatalysts: orientation transfer of photogenerated charges and their rapid interfacial reaction. *J. Mater. Chem. A* 4, 8682–8689. doi: 10.1039/C6TA02039A
- Xia, Y., and Halas, N. J. (2005). Shape-controlled synthesis and surface plasmonic properties of metallic nanostructures. *Mrs. Bull.* 30, 338–348. doi: 10.1557/mrs2005.96
- Xiang, Q., Yu, J., and Jaroniec, M. (2011). Preparation and enhanced visible-light photocatalytic H₂-production activity of graphene/C₃N₄ composites. *J. Phys. Chem. C* 115, 7355–7363. doi: 10.1021/jp200953k
- Xiao, J. Q., Lin, K. S., and Yu, Y. (2018). Novel Ag@AgCl@AgBr heterostructured nanotubes as high-performance visible-light photocatalysts for decomposition of dyes. *Catal. Today* 314, 10–19. doi: 10.1016/j.cattod.2018.04.019
- Xu, Y., Xu, H., Yan, J., Li, H., Huang, L., Xia, J., et al. (2013). A plasmonic photocatalyst of Ag/AgBr nanoparticles coupled with g-C₃N₄ with enhanced visible-light photocatalytic ability. *Colloid. Surface. A* 436, 474–483. doi: 10.1016/j.colsurfa.2013.06.005
- Xuan, N. P., Ba, M. N., Thi, H. T., and Doan, H. V. (2018). Synthesis of Ag-AgBr/Al-MCM-41 nanocomposite and its application in photocatalytic oxidative desulfurization of dibenzothiophene. *Adv. Powder Technol.* 29, 1827–1837. doi: 10.1016/j.apt.2018.04.019
- Yada, M., Inoue, Y., Sakamoto, A., Torikai, T., and Watari, T. (2014). Synthesis and controllable wettability of micro- and nanostructured titanium phosphate thin films formed on titanium plates. *ACS Appl. Mater. Inter.* 6, 7695–7704. doi: 10.1021/am500974v
- Yang, X., Tang, H., Xu, J., Antonietti, M., and Shalom, M. (2015). Silver phosphate/graphitic carbon nitride as an efficient photocatalytic tandem system for oxygen evolution. *ChemSusChem* 8, 1350–1358. doi: 10.1002/cssc.201403168
- Ye, L., Liu, J., Gong, C., Tian, L., Peng, T., and Zan, L. (2012). Two Different roles of metallic Ag on Ag/AgX/BiOX (X = Cl, Br) visible light photocatalysts: surface plasmon resonance and z-scheme bridge. *ACS Catal.* 2, 1677–1683. doi: 10.1021/cs300213m
- Zhang, L., Wang, G., Xiong, Z., Tang, H., and Jiang, C. (2018). Fabrication of flower-like direct Z-scheme β-Bi₂O₃/g-C₃N₄ photocatalyst with enhanced visible light photoactivity for Rhodamine B degradation. *Appl. Surf. Sci.* 436, 162–171. doi: 10.1016/j.apsusc.2017.11.280
- Zhang, W., Zhao, Z., Dong, F., and Zhang, Y. (2017). Solvent-assisted synthesis of porous g-C₃N₄ with efficient visible-light photocatalytic performance for NO removal. *Chin. J. Catal.* 38, 372–378. doi: 10.1016/S1872-2067(16)62585-8
- Zhang, X., Ai, Z., Falong, Jia, A., and Zhang, L. (2008). Generalized one-pot synthesis, characterization, and photocatalytic activity of hierarchical BiOX (X = Cl, Br, I) nanoplate microspheres. *J. Phys. Chem. C* 112, 747–753. doi: 10.1021/jp077471t
- Zhang, X., Li, R., Jia, M., Wang, S., Huang, Y., and Chen, C. (2015a). Degradation of ciprofloxacin in aqueous bismuth oxybromide (BiOBr) suspensions under

- visible light irradiation: a direct hole oxidation pathway. *Chem. Eng. J.* 274, 290–297. doi: 10.1016/j.cej.2015.03.077
- Zhang, Y., Gu, J., Murugananthan, M., and Zhang, Y. (2015b). Development of novel α -Fe₂O₃ /NiTiO₃ heterojunction nanofibers material with enhanced visible-light photocatalytic performance. *J. Alloy. Compd.* 630, 110–116. doi: 10.1016/j.jallcom.2014.12.193
- Zhang, Z., and Yates, J. T. (2012). Band bending in semiconductors: chemical and physical consequences at surfaces and interfaces. *Chem. Rev.* 112, 5520–5551. doi: 10.1021/cr3000626
- Zhu, Y.-P., Ma, T.-Y., Ren, T.-Z., Li, J., Du, G.-H., and Yuan, Z.-Y. (2014). Highly dispersed photoactive zinc oxide nanoparticles on mesoporous phosphonated titania hybrid. *Appl. Catal. B-Environ.* 156–157, 44–52. doi: 10.1016/j.apcatb.2014.03.001
- Zou, J. P., Wu, D. D., Luo, J., Xing, Q. J., Luo, X. B., Dong, W. H., et al. (2016). A strategy for one-pot conversion of organic pollutants into useful hydrocarbons through coupling photodegradation of MB with photoreduction of CO₂. *ACS Catal.* 6, 6861–6867. doi: 10.1021/acscatal.6b01729

Conflict of Interest Statement: The authors declare that the research was conducted in the absence of any commercial or financial relationships that could be construed as a potential conflict of interest.

Copyright © 2018 Ren, Bao, Wang, Wang and Ao. This is an open-access article distributed under the terms of the Creative Commons Attribution License (CC BY). The use, distribution or reproduction in other forums is permitted, provided the original author(s) and the copyright owner(s) are credited and that the original publication in this journal is cited, in accordance with accepted academic practice. No use, distribution or reproduction is permitted which does not comply with these terms.